Annular modes

Regressions on the annular modes (in meters)

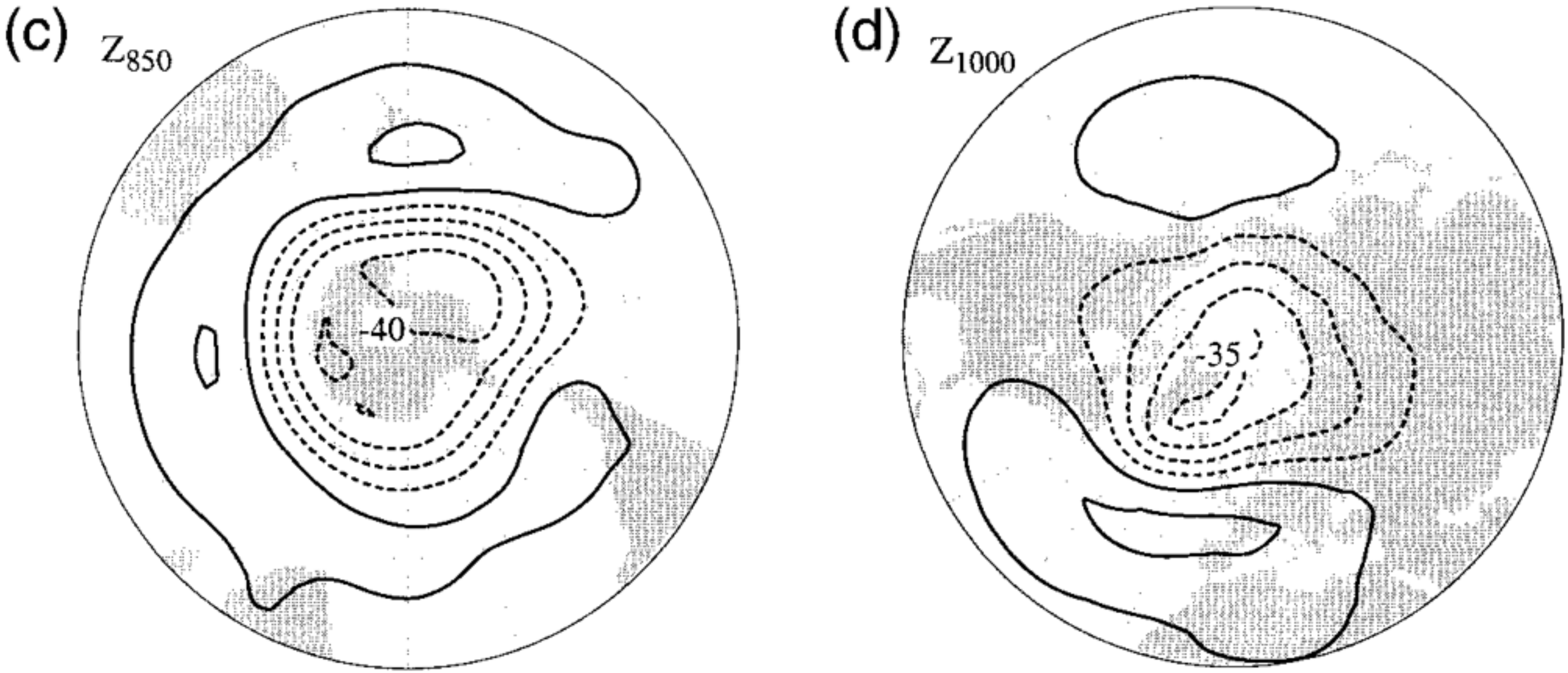

FIG. 1. (top) Zonal-mean geostrophic wind and (bottom) lower-tropospheric geopotential height regressed on the standardized indices of the annular modes (the AO and its SH counterpart) based upon monthly data, Jan 1958–Dec 1997. Left panels are for the SH, right panels are for the NH. Units are m s^{-1} (top) and m per std dev of the respective index time series (bottom). Contour intervals are 10 m (-15, -5, 5, . . .) for geopotential height and 0.5 m s^{-1} (-0.75, -0.25, 0.25) for zonal wind.

Fig. 1

Thompson and Wallace, J. Climate, 2000

Regressions of zonal-mean zonal wind on the annular modes

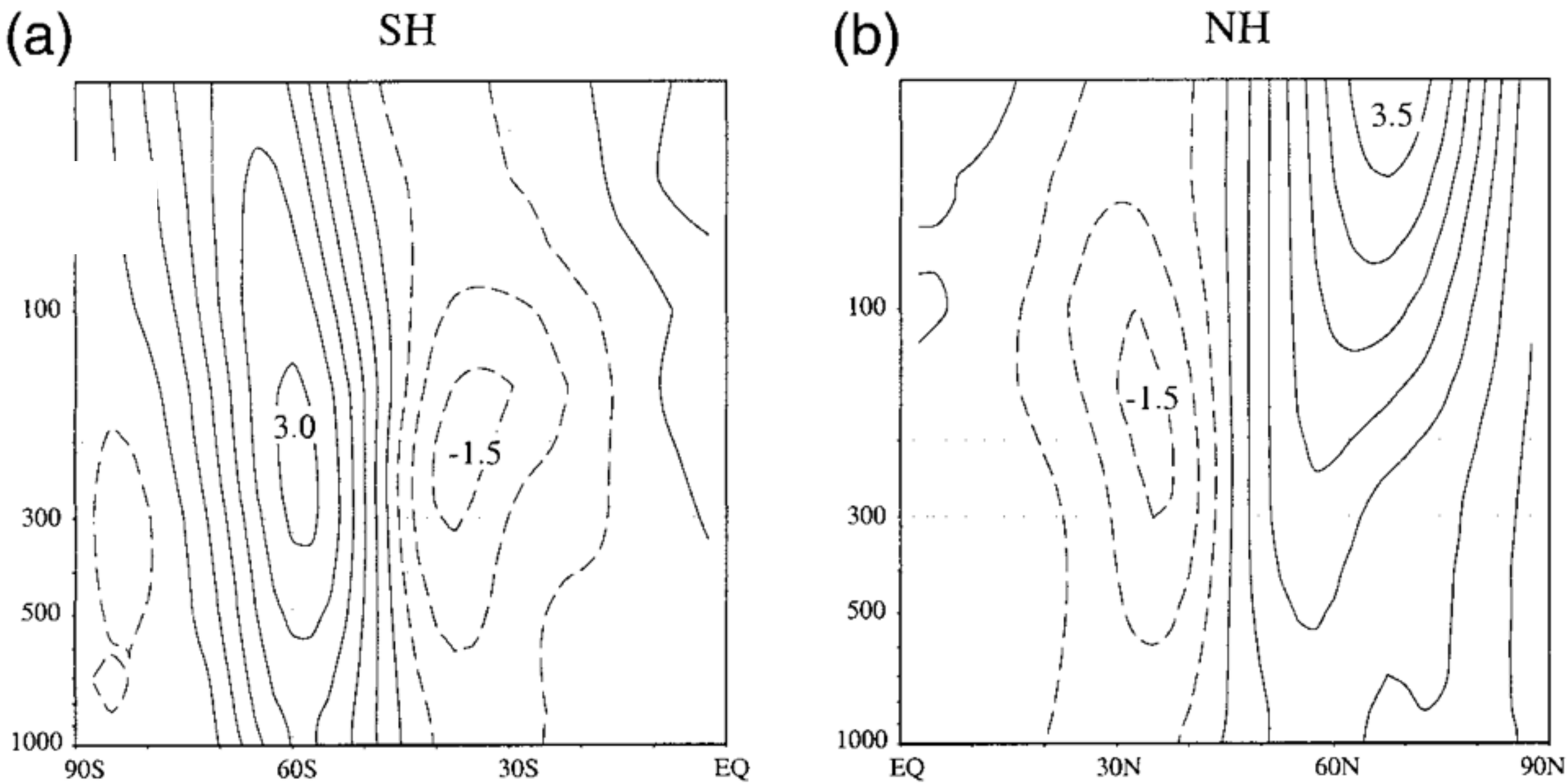

Fig. 2

FIG. 1. (top) Zonal-mean geostrophic wind and (bottom) lower-tropospheric geopotential height regressed on the standardized indices of the annular modes (the AO and its SH counterpart) based upon monthly data, Jan 1958–Dec 1997. Left panels are for the SH, right panels are for the NH. Units are m s^{-1} (top) and m per std dev of the respective index time series (bottom). Contour intervals are 10 m (-15, -5, 5, . . .) for geopotential height and 0.5 m s^{-1} (-0.75, -0.25, 0.25) for zonal wind.

Thompson and Wallace, J. Climate, 2000

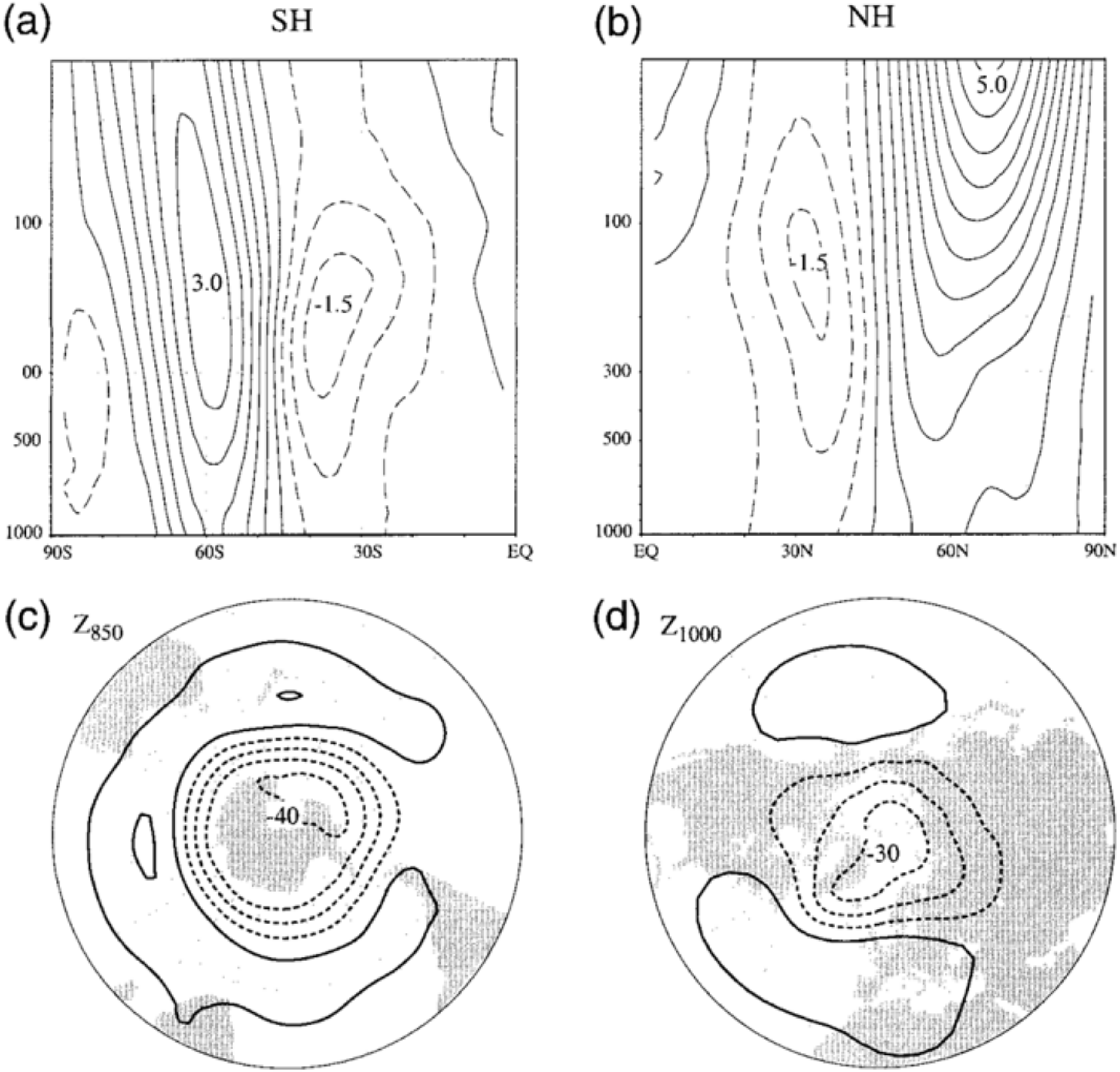

Fig. 3

FIG. 3. As in Fig. 1, but regression maps are based on the standardized leading PC time series of the zonal-mean geopotential height field (1000–50 hPa; 20°–90°).

Thompson and Wallace, J. Climate, 2000

‘Variance explained’ by leading modes

TABLE 2. Percentage of variance explained by the leading modes in EOF expansion of monthly mean fields for the region poleward of 20°, based on data for all calendar months: mode 1 (2, 3).

	Zonally varying SLP (NH) and Z_{850} (SH)	Zonal-mean geopotential height (1000 to 50 hPa)	Zonal-mean zonal wind (1000 to 50 hPa)
NH	20 (10, 10)	45 (17, 12)	35 (24, 12)
SH	27 (12, 9)	47 (27, 10)	45 (22, 9)

Fig. 4

Thompson and Wallace, J. Climate, 2000

Example of time series of Arctic Oscillation in winter

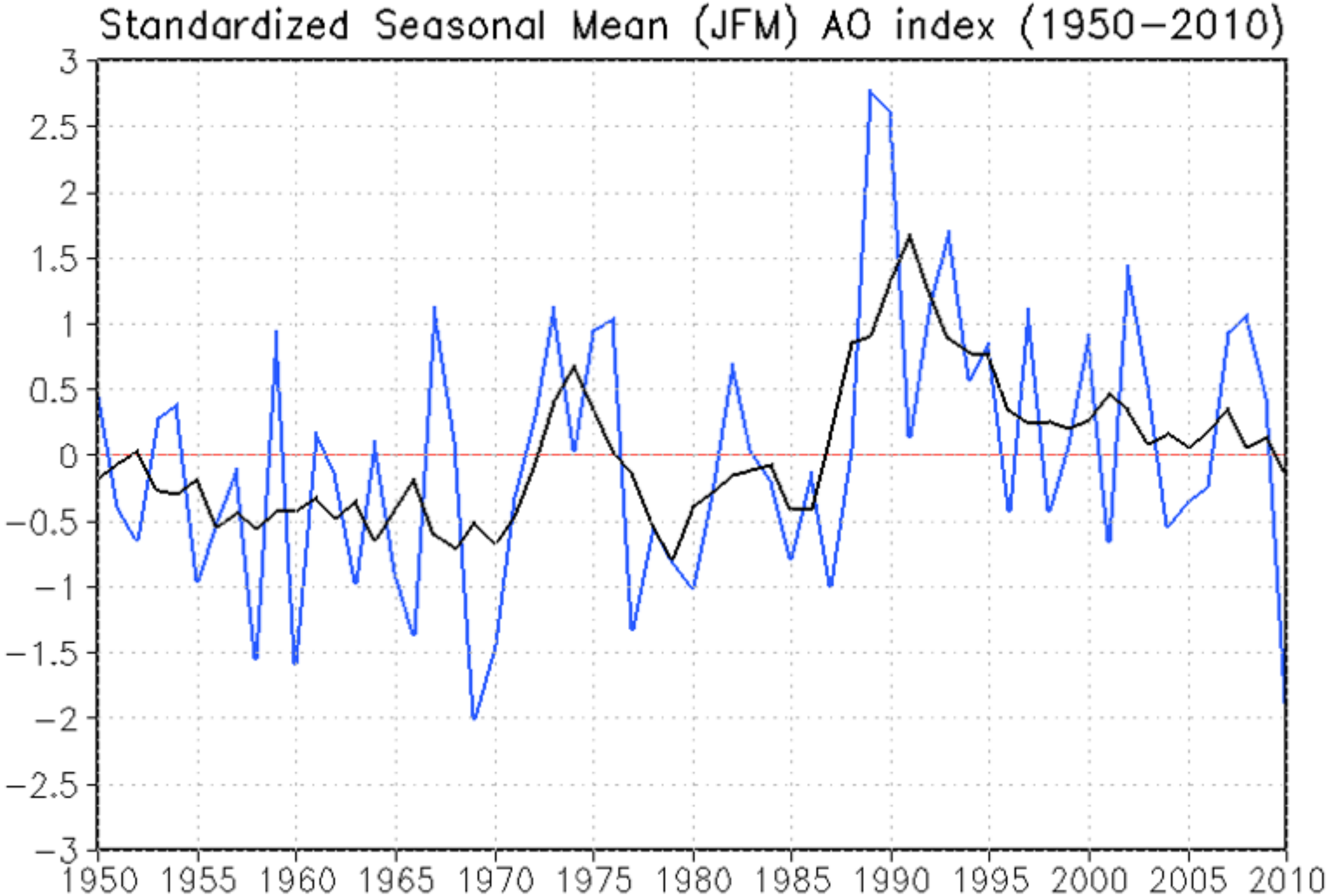

The standardized seasonal mean AO index during cold season (blue line) is constructed by averaging the daily AO index for January, February and March for each year. The black line denotes the standardized five-year running mean of the index. Bith curves are standardized using 1950-2000 base period statistics.

Fig. 5

www.cpc.noaa.gov/products/precip/CWlink/daily_ao_index/JFM_season_ao_index.shtml

Power spectrum is similar to that of a red-noise process

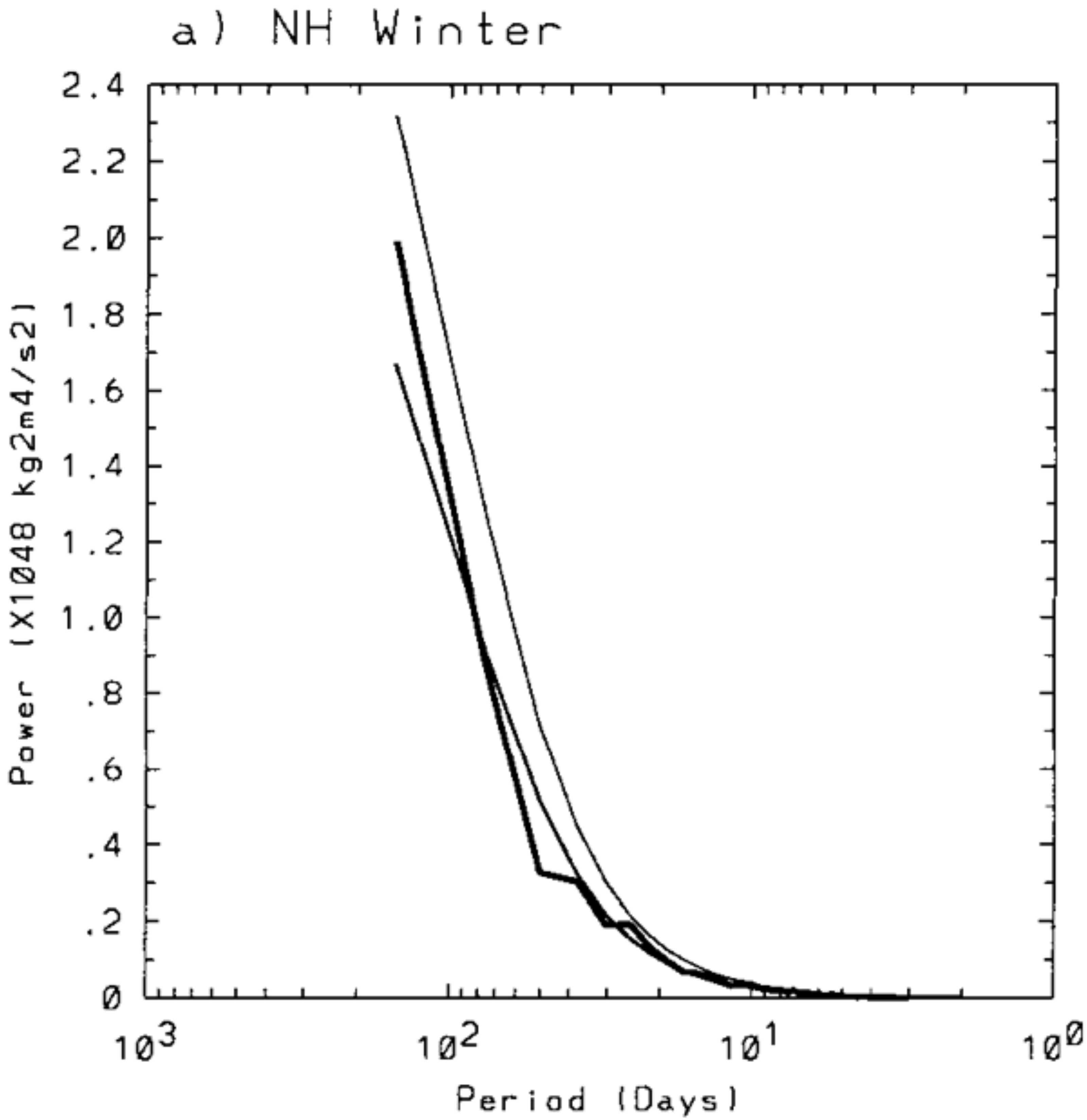

Fig. 6

Feldstein, J. Climate, 2000

FIG. 4. Power spectra for the intraseasonal ZI time series for (a) the NH winter, (b) the NH summer, (c) the SH winter, and (d) the SH summer. The corresponding red noise spectra and 95% confidence levels are also shown.

Lower-tropospheric temperature patterns associated with annular modes

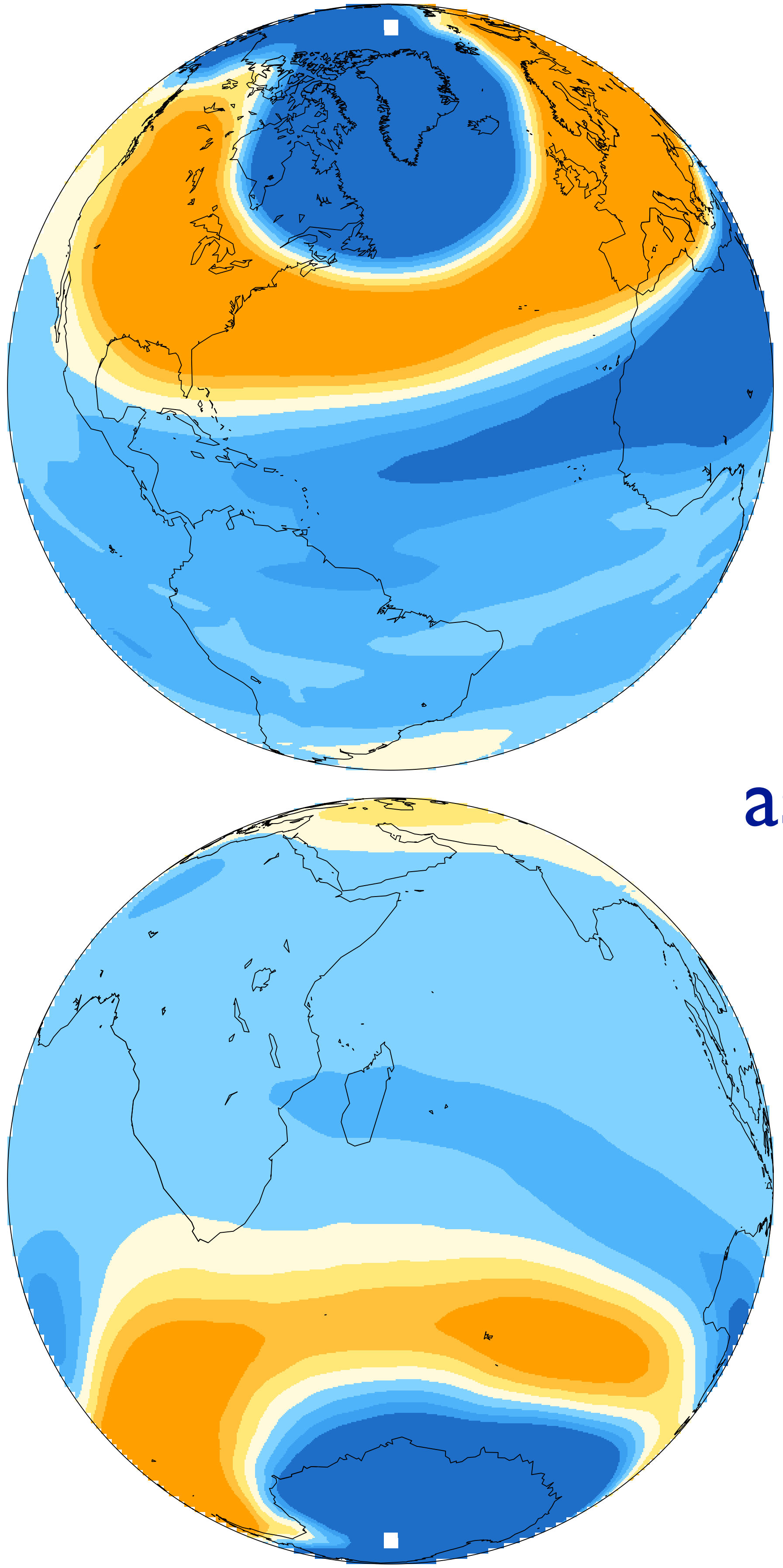

MSU2LT data regressed on the JFM NAM index (top) and the SAM index (bottom). Contour interval 0.1 K/std.

Wallace, On the Arctic and Antarctic Oscillations, 2000

Fig. 7

Summary of AO in its high index state: anomalous eddy momentum fluxes and Ferrel cell help maintain the high index state for a while

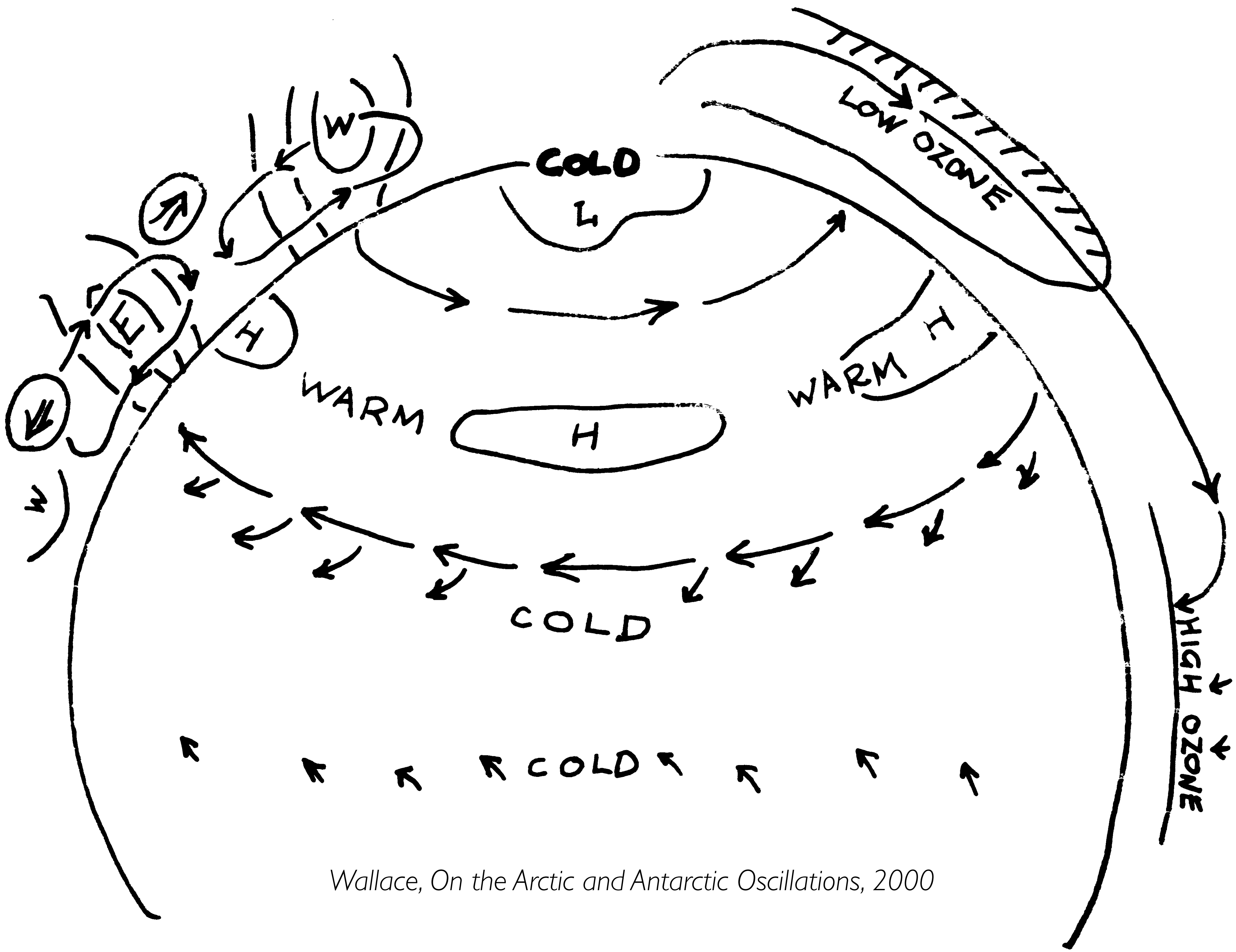

Fig. 8

Wallace, On the Arctic and Antarctic Oscillations, 2000

Blocking and severe winter weather modulated by AO

Number of JFM days 1958-97 marked by blocking events

Location	Total	High AO	Low AO
Alaska (140°W-180°W; 65°N-75°N)	389	46	98
North Atlantic (20°W- 50°W; 55°N-65°N)	350	0	195
Russia (50°E-70°E; 60°N-70°N)	428	32	85

Wallace, On the Arctic and Antarctic Oscillations, 2000

Fig. 9

Blocking and severe winter weather modulated by AO

Number of JFM days 1958-97 with minimum temperatures <

Location	Total	High AO	Low AO
< -15° C in Yakima, WA.	116	17	41
< -20° C in Chicago, Il.	181	12	50
< -1° C in Orlando, Fl.	108	11	27
< -5° C in Paris, France	142	8	54
< -33° C in Novosibirsk	120	7	46
< -20° C in Beijing, Ch.	141	11	41
< -2° C in Tokyo, Japan	140	7	40

Wallace, On the Arctic and Antarctic Oscillations, 2000

Fig. 10

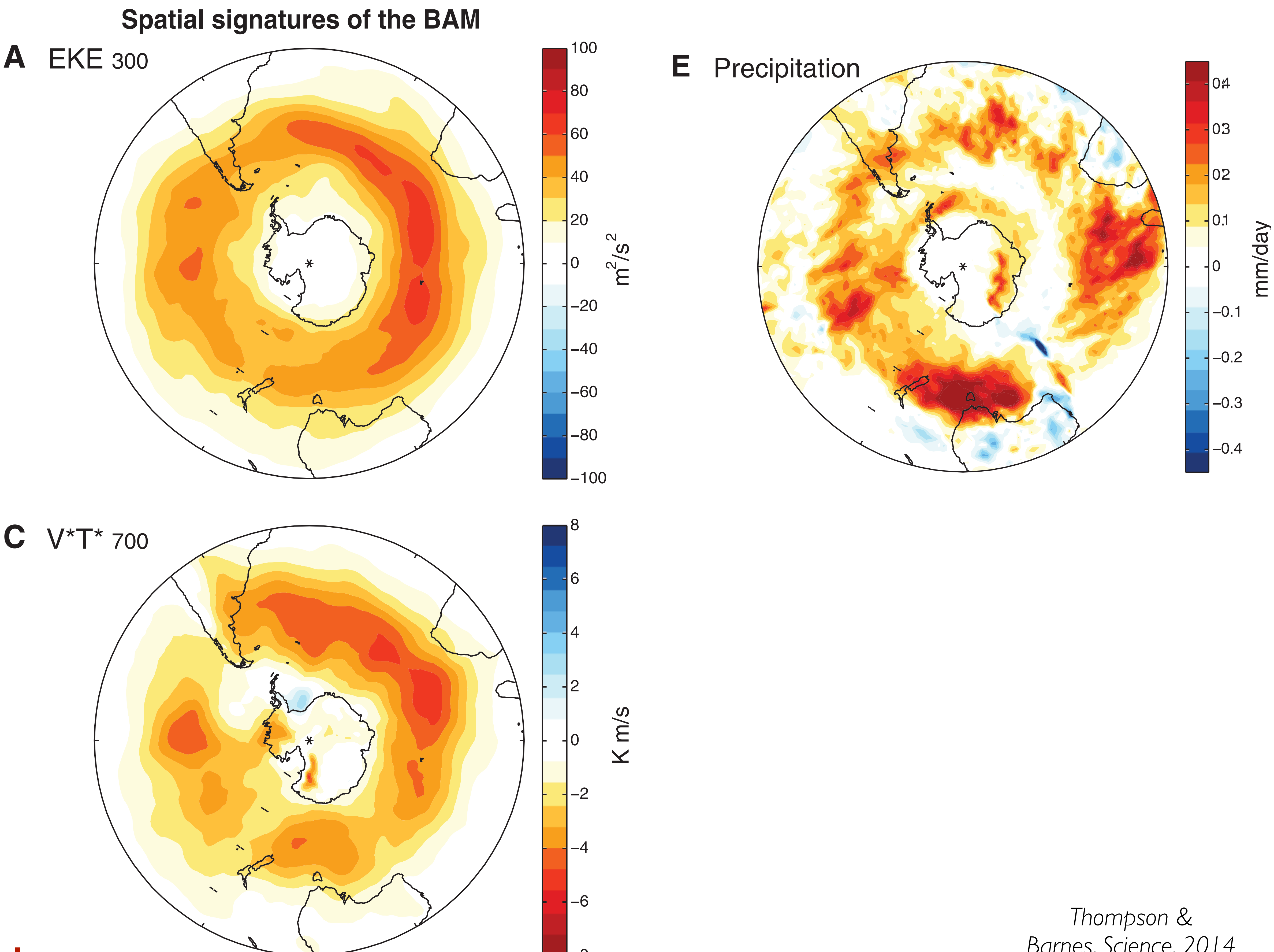

Thompson & Barnes, Science, 2014

Fig. 11

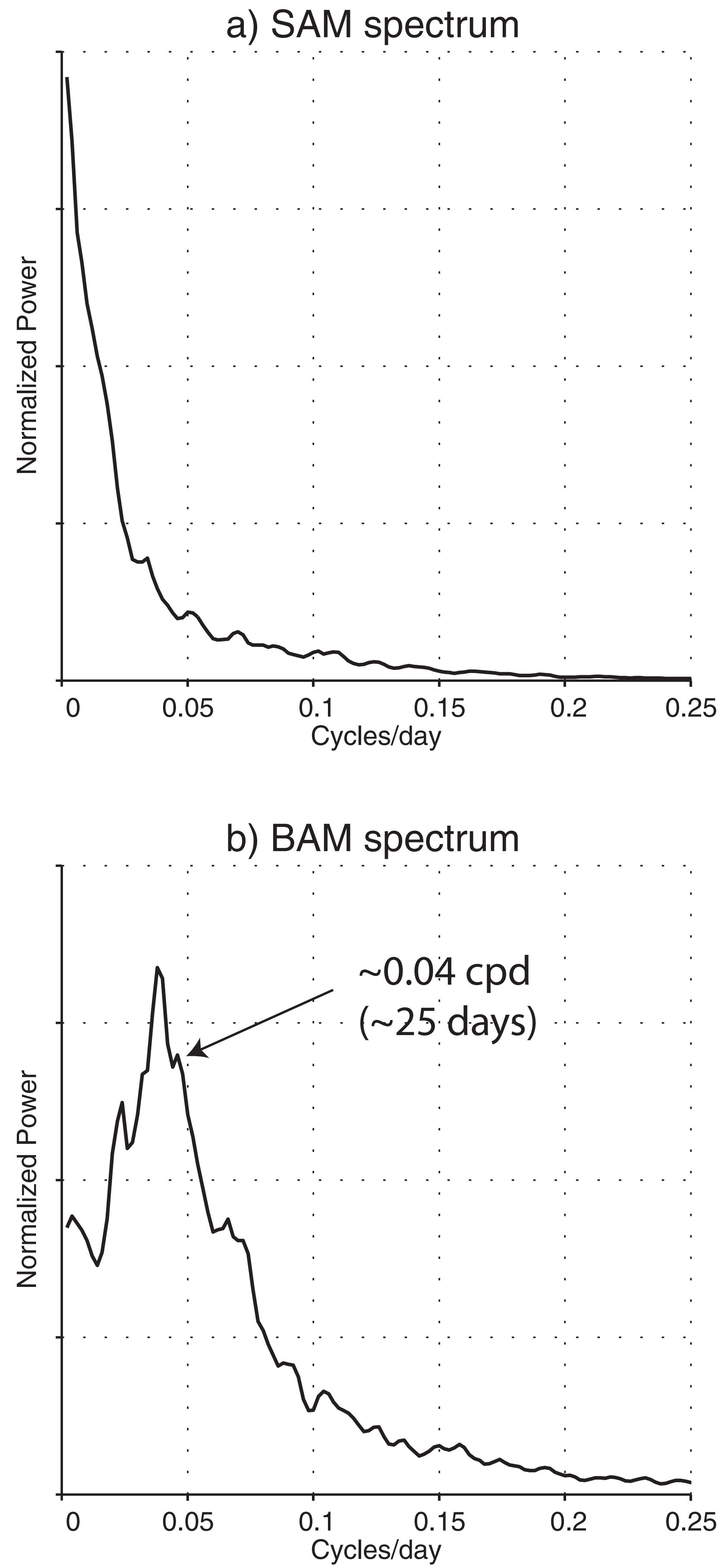

FIG. 12. Power spectra of the SAM and BAM indices. See text for details of the calculations.

SAM resembles a red-noise process

BAM exhibits periodic variability (~25 days)

Thompson & Woodworth, JAS, 2014

Fig. 12

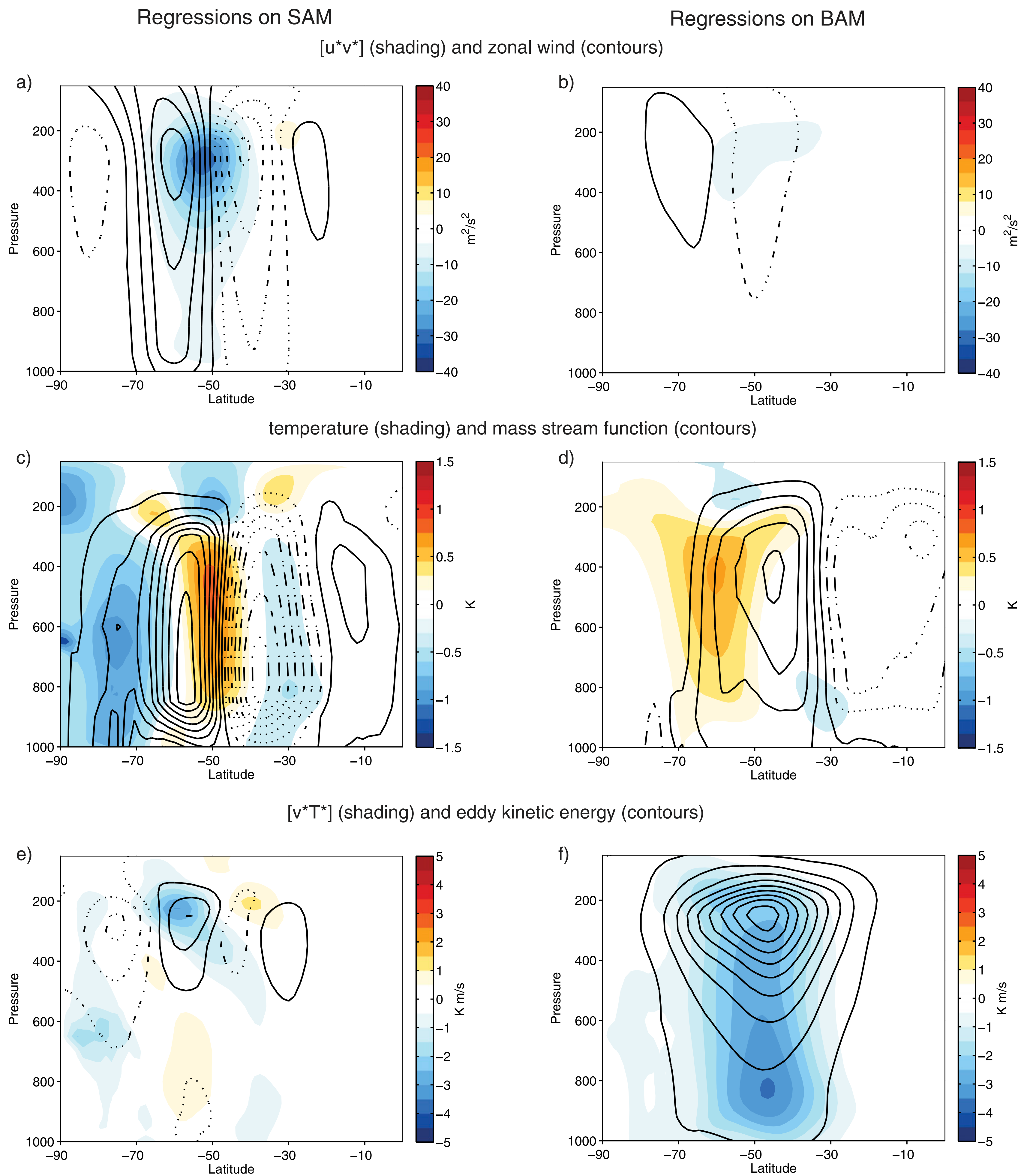

Thompson & Woodworth, JAS, 2014 based on ERA-interim

Fig. 13

Regressions on Southern Hemisphere mean [V*T*]

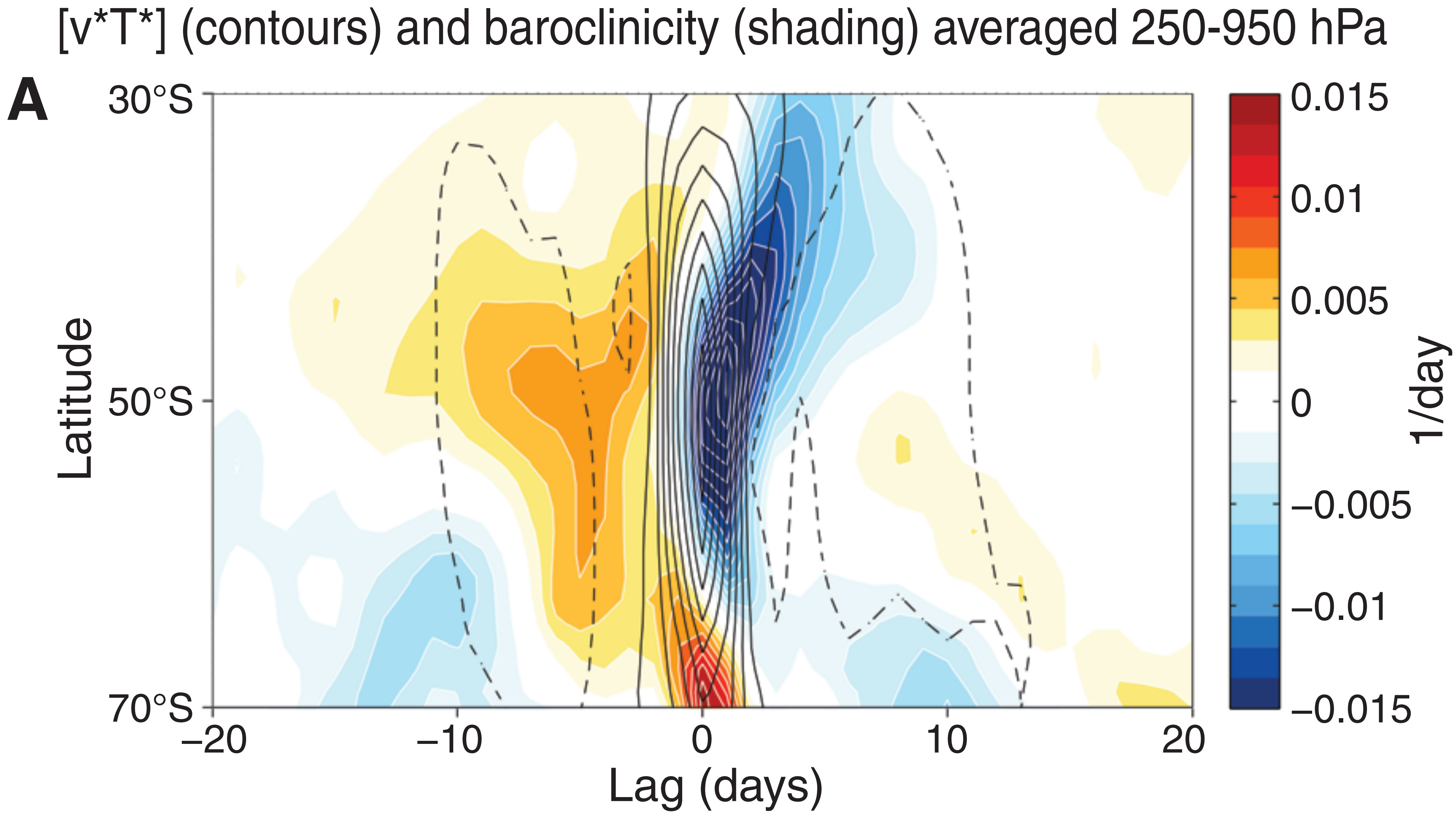

Strong baroclinicity, followed by strong heat flux, followed by weak baroclinicity

Thompson & Barnes, Science, 2014

Fig. 14

Comparison of simple stochastic model with ERA-interim for power spectrum of heat flux

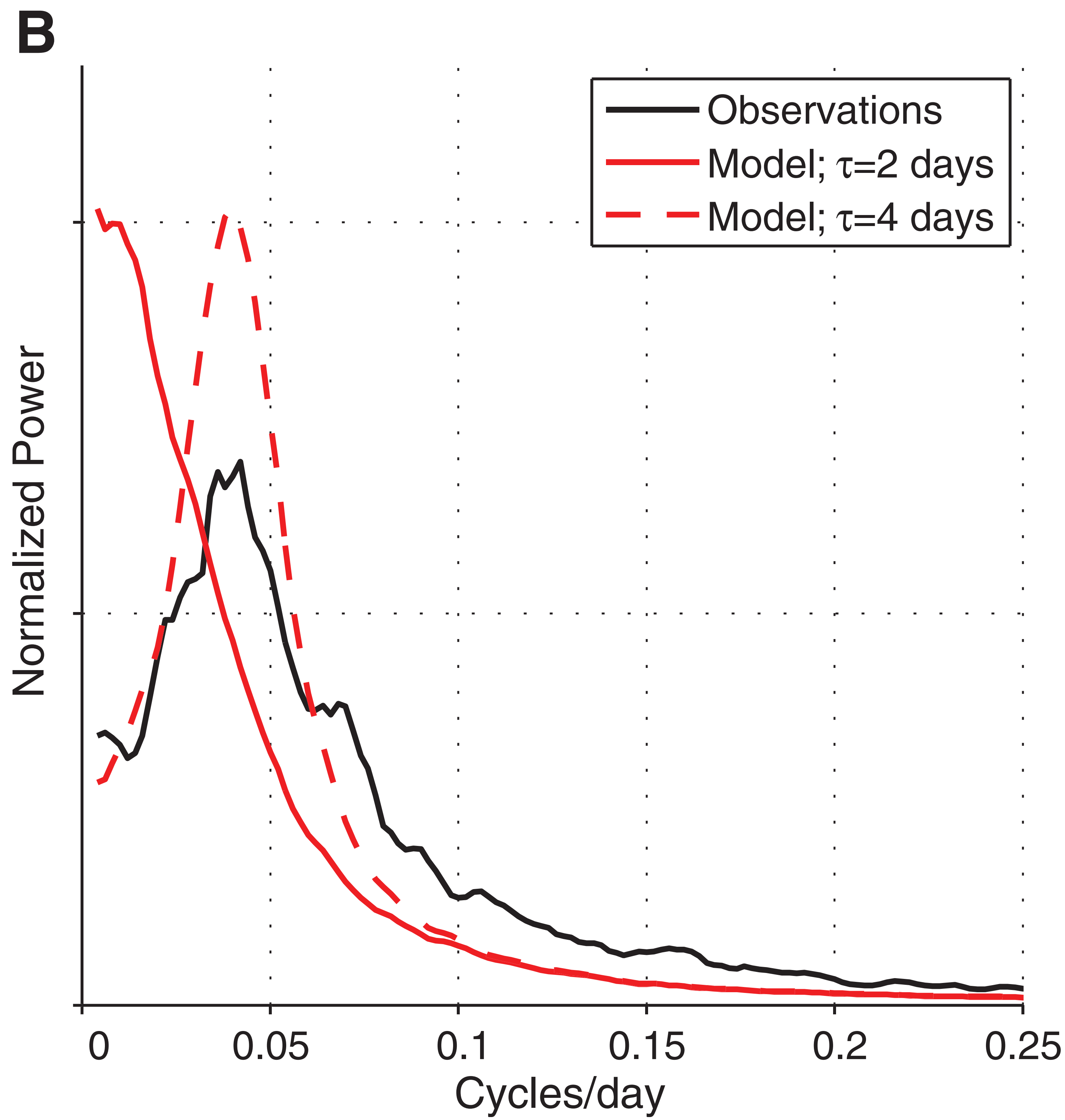

Thompson & Barnes, Science, 2014

Fig. 15